

PAPER • OPEN ACCESS

Search for the $K_L \rightarrow \pi^0 \gamma$ decay in the KOTO experiment

To cite this article: N Shimizu and for the KOTO collaboration 2020 *J. Phys.: Conf. Ser.* **1526** 012018

View the [article online](#) for updates and enhancements.

You may also like

- [Development of a PMT base used for the new charged veto detector in the J-PARC KOTO experiment](#)
Ayumu Kitagawa
- [Status of KOTO Experiment at J-PARC](#)
Manabu Togawa
- [A new cylindrical photon-veto detector for the KOTO experiment](#)
Manabu Togawa



ECS
The
Electrochemical
Society
Advancing solid state &
electrochemical science & technology

DISCOVER
how sustainability
intersects with
electrochemistry & solid
state science research

Search for the $K_L \rightarrow \pi^0 \gamma$ decay in the KOTO experiment

N Shimizu for the KOTO collaboration

Department of Physics, Osaka University, Toyonaka, Osaka 560-0043, Japan

E-mail: shimizu@champ.hep.sci.osaka-u.ac.jp

Abstract. We report a preliminary result of a new search for the $K_L \rightarrow \pi^0 \gamma$ decay, which is forbidden by the Lorentz invariance and gauge principle. The search was carried out using the data obtained from 2016 to 2018 at the J-PARC proton beam facility using the KOTO detector. The achieved single event sensitivity was $(6.9 \pm 0.3_{\text{stat.}} \pm 1.5_{\text{syst.}}) \times 10^{-8}$. No signal candidate was found in the signal region and the upper limit was set to $\mathcal{B}(K_L \rightarrow \pi^0 \gamma) < 1.7 \times 10^{-7}$ at the 90% confidence level.

1. Introduction

The $K_L \rightarrow \pi^0 \gamma$ decay is forbidden by the Lorentz invariance and the gauge principle. In the K_L rest frame, the spin of a massless photon must have a polarization along the decay axis, but the back-to-back configuration cannot produce the parallel component of the orbital angular momentum. In addition, the $K_L \rightarrow \pi^0 \gamma$ decay violates charge and parity symmetry (CP), and the flavor changing neutral transition $s \rightarrow d$ is heavily suppressed in the Standard Model (SM). Such restrictions on the $K_L \rightarrow \pi^0 \gamma$ decay provide the opportunity to search for physics beyond the SM. In particular, as Ref. [1] suggests, the test of Lorentz invariance should be experimentally confirmed in high energy system as often studied in spectroscopic systems [2, 3]. There are several scenarios that predict nonzero probability of $K_L \rightarrow \pi^0 \gamma$ decay [4, 5].

2. KOTO experiment

The KOTO experiment is carried out at the Hadron Experimental Facility of J-PARC, Ibaraki Japan, using the high intensity 30 GeV proton accelerator. The neutral K_L beam is produced by protons hitting a target, and transported into the KOTO detector with an angle of 16° from the primary beam line. Meanwhile, charged particles and other neutral particles, such as neutrons, short-lived neutral kaon K_S , and γ 's, are removed by a sweeping magnet and a lead absorber. The flux of the K_L beam is $N_{K_L} = 4.7 \times 10^7 / 2 \times 10^{14}$ protons on target (POT) at the entrance of the detector.

The principal goal of the KOTO experiment is to search for the $K_L \rightarrow \pi^0 \nu \bar{\nu}$ decay, which is heavily suppressed in the SM ($\mathcal{B}(K_L \rightarrow \pi^0 \nu \bar{\nu}) = (3.0 \pm 0.3) \times 10^{-11}$ [6]). The experimental signature of $K_L \rightarrow \pi^0 \nu \bar{\nu}$ is $2\gamma + \text{nothing}$. Hence, the KOTO detector consists of an electromagnetic calorimeter and hermetic veto counters. The apparatus is ideal to search for the $K_L \rightarrow \pi^0 \gamma$ decay as well.

Figure 1 shows the sectional view of the KOTO detector. The K_L decays in the central region of the detector (decay volume), which is kept in high vacuum (10^{-5} Pa) to suppress interactions



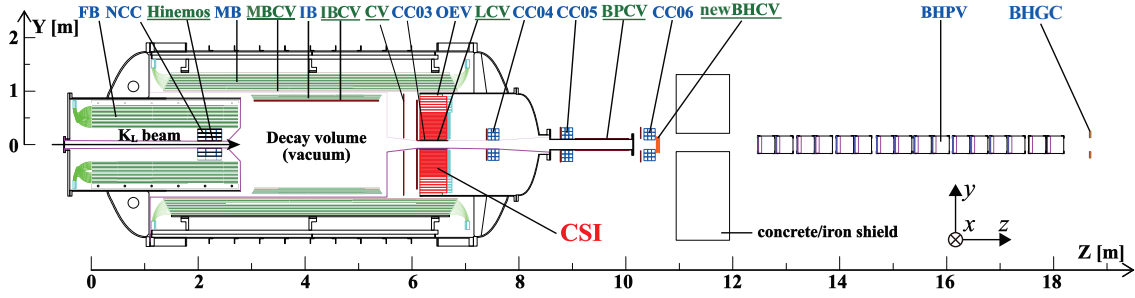


Figure 1: Sectional view of the KOTO detector. The K_L beam, pointing to $+z$ direction in the figure, is transported from the left side and the decay region is kept in high vacuum (10^{-5} Pa). The energy and position of γ 's from the K_L decay are measured by the CsI crystals (red) and other decay products are detected by hermetic veto counters (green).

of neutrons in the beam. The energies and position of photons from K_L decays are measured with the calorimeter which is made of 2716 50-cm-long Cesium Iodide (CsI) crystals. Other extra particles are vetoed by hermetic lead-scintillator detectors (FB, MB, and IB). To veto charged particles, the inner surfaces of IB, MB, and the beam hole of the calorimeter are covered with 5-mm-thick plastic scintillators (IBCV, MBCV, and LCV). Charged particles entering the CsI calorimeter are vetoed by the two layers of 3-mm-thick plastic scintillation counters (CV) placed upstream of the calorimeter. To veto charged particles escaping from the beam hole of the CsI calorimeter, three layers of wire chambers are placed downstream of the calorimeter in beam (newBHCV). To veto photons passing through the beam hole at the center of the CsI calorimeter, there are four types of *collar*-shaped undoped CsI counters (CC03, CC04, CC05, and CC06). To veto photons which stay in the beam, sixteen modules, made of lead and aerogel (BHPV), are placed downstream of calorimeter [7]. To veto particles = decaying towards upstream, a detector made of undoped CsI crystals (NCC) is placed near the downstream end of FB. The details of these detectors are available in Ref. [8].

3. Data collection

The data was taken in June 2016, June to August 2017, and January 2018. During these periods, the proton beam power increased from 22 to 44 kW. The trigger required energy deposit in the CsI calorimeter > 550 MeV and no large signals in IB, MB, CC03, CV, and NCC. The energy thresholds for veto counters were set sufficiently larger than the thresholds for the offline analysis. The number of clusters were calculated with an online hardware logic and events having two or three or four or six clusters were recorded [9]. This analysis used data corresponding to 2.8×10^{18} POT. The detail of DAQ is available in Ref. [10].

4. Reconstruction of the $K_L \rightarrow \pi^0 \gamma$ decay

The candidate of the $K_L \rightarrow \pi^0 \gamma$ event was required to have exactly three γ clusters (γ_0, γ_1 , and γ_2 , where 1, 2 are indices of γ 's produced from the π^0) in the CsI calorimeter. The cluster was reconstructed by integrating the CsI crystals with > 3 MeV. The vertex position of the π^0 production point $z = z_{\text{vtx}}^{\pi^0}$ was reconstructed assuming that it was on the beam axis and that the invariant mass, $M_{\gamma_1 \gamma_2}$, equals the mass of the neutral pion. The K_L decay position, $z = z_{\text{vtx}}^{K_L}$, was similarly formed by requiring that the three γ 's to have the nominal mass of K_L . The difference of the two vertices, $\Delta z_{\text{vtx}} = z_{\text{vtx}}^{\pi^0} - z_{\text{vtx}}^{K_L}$ should be small for the signal events; we thus chose the combination of the photons by selecting the pair which had the smallest $|\Delta z_{\text{vtx}}|$ value.

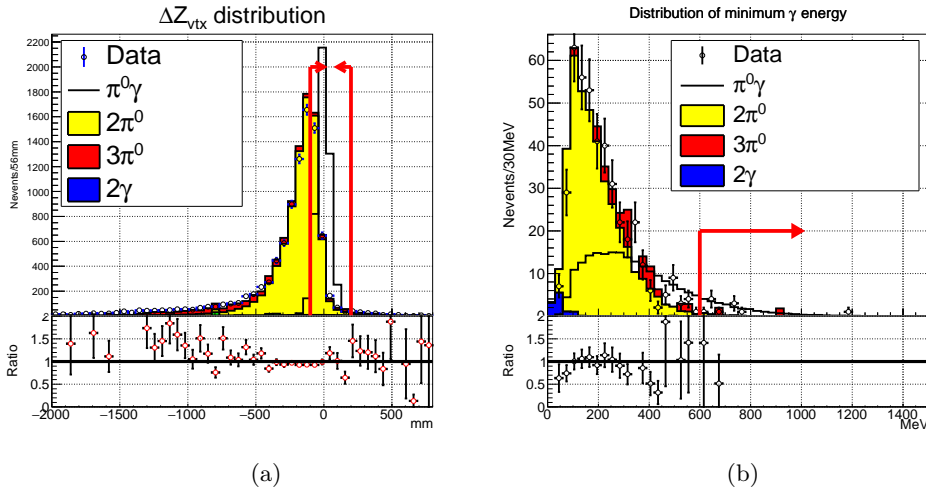


Figure 2: (a) Distribution of Δz_{vtx} after all vetoes, cluster shape cut (b) distribution of the minimum energy of three γ 's after all vetoes, cluster shape cut, Δz_{vtx} , and $490 < M_{\pi^0\gamma}/\text{MeV} < 520$ requirements: points (data), $K_L \rightarrow 2\pi^0$ (yellow), $K_L \rightarrow 3\pi^0$ (red), and $K_L \rightarrow \pi^0\gamma$ (black). Signal histogram is not stacked and its branching ratio is assumed to be $\mathcal{B}(K_L \rightarrow \pi^0\gamma) = \mathcal{B}(K_L \rightarrow 2\pi^0) \times 0.01 = 8.64 \times 10^{-6}$ [11]. Red arrow represents the selection criteria of $E > 600$ MeV.

The four momenta of three γ 's were reconstructed assuming the production point of $z = z_{vtx}^{\pi^0}$ on the beam axis. The invariant mass of the reconstructed π^0 and γ , $M_{\pi^0\gamma}$, was then calculated.

5. Event selection and background estimation

To avoid human bias, we adopted the blind analysis technique; the *signal region* (SR) was defined in the two-dimension space of $(z_{vtx}^{\pi^0}, M_{\pi^0\gamma})$, and the selection criteria were determined without looking at the events in the SR. The SR was defined to be $1500 < z_{vtx}^{\pi^0}/\text{mm} < 3500$ and $490 < M_{\pi^0\gamma}/\text{MeV} < 520$ (see Fig.3). The other regions were used as control regions (CRs). In particular, the lower right region (referred to as CR2), defined as $3500 < z_{vtx}^{\pi^0}/\text{mm} < 6200$ and $400 < M_{\pi^0\gamma}/\text{MeV} < 490$, is dominated by the $K_L \rightarrow 2\pi^0$ decays and thus we used the number of entries in CR2 to get the K_L yield. To select the $K_L \rightarrow \pi^0\gamma$ signal, we required $-100 < \Delta z_{vtx}/\text{mm} < 200$ as shown in Fig. 2a.

The cluster shape based on energy deposit in each crystal was compared with the one of γ generated by MC to compute a χ^2 value. We required all the γ cluster candidates to satisfy $\chi^2 < 5$. Moreover, a neural network was used to distinguish γ clusters from neutron clusters based on the information of two-dimensional cluster shape, relative energies of crystals, energy-weighted xy -position of the cluster, and γ 's incident angle. All the γ 's were required to have the likelihood of more than 0.8, which corresponds to 90% and 3% efficiencies for γ 's and neutrons, respectively. The requirement also discriminates overlapping photons.

To suppress other K_L decays, we required no significant on-time signals in veto detectors. In particular, to exclude $K_L \rightarrow 2\pi^0$ decay mode, we required < 1 MeV energy deposits in the three barrel counters. In addition, all the photons hitting the calorimeter were required to have more than 600 MeV as shown in Fig. 2b. Figures 3a and 3b show the $(z_{vtx}^{\pi^0}, M_{\pi^0\gamma})$ distributions after applying the selection criteria described above for the signal and Monte Carlo backgrounds, respectively.

Table 1 summarizes the expected number of background events in the SR. Of all the

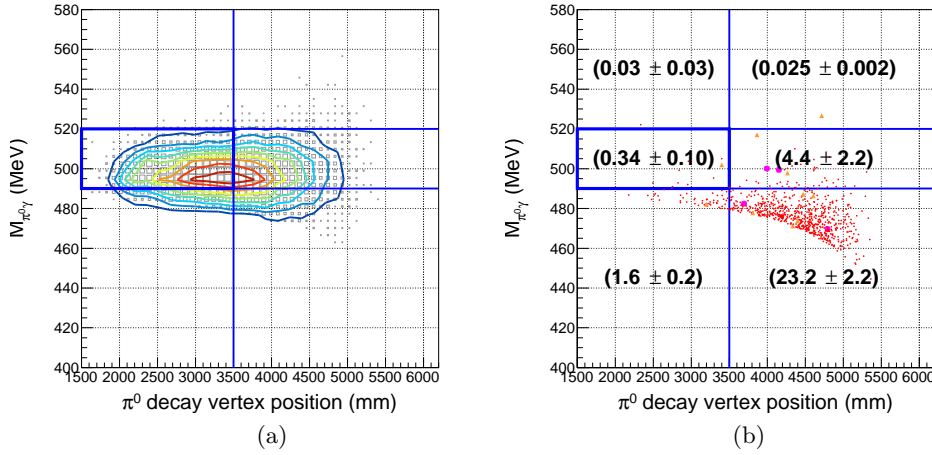


Figure 3: Correlation plots of $z_{\text{vtx}}^{\pi^0} - M_{\pi^0\gamma}$ by MC simulation: (a) signal ($K_L \rightarrow \pi^0\gamma$), (b) backgrounds. In (b), the rectangle, circular, and triangular markers represent $K_L \rightarrow 2\pi^0$, $K_L \rightarrow 3\pi^0$, and $K_L \rightarrow \pi^0\gamma\gamma$ events, respectively. The number of markers do not have the same weights.

background sources, the $K_L \rightarrow 2\pi^0$ mode exhibits the largest contribution after applying all the selection criteria. The decay mode can be a background if a small energy photon escaped from the detection in the veto counters. Also, if two photon clusters fuse, this can be a source of background. For the $K_L \rightarrow 2\pi^0$ events, the contributions in the SR b_s was estimated by:

$$b_s = b_c \times \frac{N_s^{\text{MC}}}{N_c^{\text{MC}}}, \quad (1)$$

where b_c is the number of the observed events in the CR2 under the loosened energy threshold of γ 's ($E > 300$ MeV), and N_i ($i = s, c$) is the corresponding estimations by the MC simulation. The purity of the $K_L \rightarrow 2\pi^0$ events in b_c was $\sim 99\%$.

Because it was difficult to produce sufficient amount of $K_L \rightarrow 3\pi^0$ MC events, the number of $K_L \rightarrow 3\pi^0$ events in the SR was estimated with a data-driven approach. Similarly to the $K_L \rightarrow 2\pi^0$ case, we selected a control region dominated by the $K_L \rightarrow 3\pi^0$ decays defined with $\sqrt{M_{\gamma_0\gamma_1}^2 + M_{\gamma_0\gamma_2}^2} > 490$ MeV, where $M_{i,j} = \sqrt{(p_i + p_j)^2}$, and p_i ($i = 0, 1, 2$) are four-momenta of three γ 's. Using the number of events in the control region, b_c , we estimated the number of events in the SR. Because $N_s^{\text{MC}} = 0$, we assigned as an upper limit $b_s < 0.5$ at the 68% C.L.

If an accidental hit on the calorimeter is associated by the $K_L \rightarrow 2\gamma$ decay, it can become a background. We generated MC samples of $K_L \rightarrow 2\gamma$ decay, corresponding to 18 times the experimental data, but no events satisfied the selection criteria.

If a π^0 is produced by the interaction of beam halo neutrons in the NCC, and the two photons from the π^0 are observed with an accidental hit in the CsI calorimeter, this can be a background. We produced a dedicated MC sample and studied the number of remaining events in the SR. The Δz_{vtx} requirement suppressed to be less than 0.02 events at the 68% C.L.

The $K_L \rightarrow \pi^0\gamma\gamma$ decay mode can be an irreducible background to $K_L \rightarrow \pi^0\gamma$ process, if one of γ energy becomes soft in the laboratory frame. However, its small branching fraction of $\mathcal{B}(K_L \rightarrow \pi^0\gamma\gamma) = 1.27 \times 10^{-6}$ [11] gives small impact.

We also considered the contributions from other K_L decays having charged particles in the final state. The strong rejection capability of the charged particles by CV suppresses the contributions in the SR to be less than 0.04 events at the 68% C.L.

Table 1: Expected number of backgrounds in Signal Region (SR). Upper limit is 68% C.L..

Source	Entries
$K_L \rightarrow 2\pi^0$	0.32 ± 0.10
$K_L \rightarrow 3\pi^0$	< 0.5
$K_L \rightarrow 2\gamma$	< 0.06
Neutron	< 0.02
$K_L \rightarrow \pi^0\gamma\gamma$	0.02 ± 0.002
Other K_L decays	< 0.04
Total	$0.34 \pm 0.1 (< 1.0)$

Table 2: List of systematic contributions on the SES (%)

Source	(%)
Veto	17
Kinematic selection	12
Statistics for normalization	4.4
Online veto	6.4
Trigger	1.8
Cluster shape	1.5
Geometrical	1.5
Clustering	1.0
Reconstruction	0.3
$\mathcal{B}(K_L \rightarrow 2\pi^0)$	0.6
Total	$4.4_{\text{stat.}} \oplus 22_{\text{syst.}}$

6. Method and evaluation of systematic uncertainty of the sensitivity

The branching fraction of the signal was measured as a ratio between the numbers of events in SR and CR2:

$$\mathcal{B}(K_L \rightarrow \pi^0\gamma) = N_{obs}^{\text{SR}} \cdot \text{SES} \equiv N_{obs}^{\text{SR}} \cdot \frac{1}{N_{obs}^{\text{CR2}}} \cdot \frac{\epsilon_{2\pi^0}^{\text{CR2}}}{\epsilon_{\pi^0\gamma}^{\text{SR}}} \cdot \mathcal{B}(K_L \rightarrow 2\pi^0), \quad (2)$$

where N_{obs}^{SR} and $N_{obs}^{\text{CR2}} = 528$ are the numbers of the events in the SR and CR2 (under the condition of $E > 300$ MeV), respectively, $\epsilon_{\pi^0\gamma}^{\text{SR}} = 2.1 \times 10^{-5}$ and $\epsilon_{2\pi^0}^{\text{CR2}} = 8.9 \times 10^{-7}$ are the acceptances (from Monte Carlo) of the signal and the $K_L \rightarrow 2\pi^0$ events in each region, respectively, $\mathcal{B}(K_L \rightarrow 2\pi^0) = 8.6 \times 10^{-4}$ is the branching ratio of the $K_L \rightarrow 2\pi^0$ decay, and $\text{SES} = (6.9 \pm 0.3_{\text{stat.}} \pm 1.5_{\text{syst.}}) \times 10^{-8}$ is a factor called the *single event sensitivity*.

Table 2 summarizes the various sources of the systematic uncertainties on the SES. The total uncertainty was estimated to be 22%. The largest contribution comes from the limited knowledge of the acceptance of veto detectors. We evaluated the ratios of the acceptances between data and MC in the CR2 region and assigned the quadratic sum of the residuals from unity as systematic uncertainty. The second largest effect comes from the systematic uncertainty due to the acceptance of kinematic selection. Similarly to vetoes, the acceptances of data and MC were compared. This uncertainty is mainly caused by the limited statistics of data used for this evaluation. The same situation holds for the evaluation of the normalization. We observed a systematic effect from the online veto, which was caused by the different veto energy thresholds between online hardware and offline software. This was due to the intentionally-loosened offline veto energy threshold to minimize the acceptance loss by the accidental hits in the CV, since the charged decay modes contribute less to the SR. Other effects, such as a trigger, cluster-shape discrimination, geometrical acceptance, clustering, and reconstruction are smaller than the above. The uncertainty of the branching ratio of $K_L \rightarrow 2\pi^0$ was taken from the PDG value [11].

7. Result

After determining the selection criteria described above, we unmasked the SR and found no signal candidates as shown in Fig. 4. The large discrepancy in the upper right region can be explained by the limited statistics of the simulation of $K_L \rightarrow 3\pi^0$ decays. When we loosened the minimum photon energy cut ($E > 600$ MeV \rightarrow $E > 300$ MeV), the contribution from the $K_L \rightarrow 3\pi^0$ decays by Monte Carlo simulation is 17 ± 5 and this is consistent with the observation of 18. The

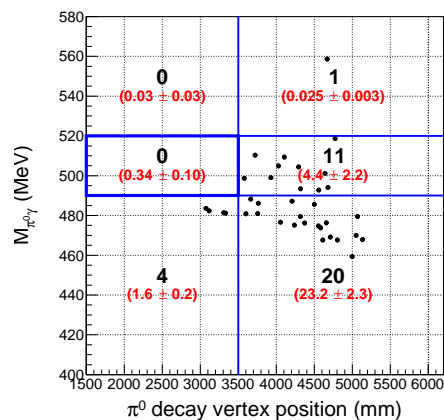


Figure 4: Scattering plot of $z_{vtx}^{\pi^0}$ vs $M_{\pi^0\gamma}$ of data. Black values are the numbers of the observed events and red ones are predictions by the MC simulation.

observed number of events in the SR is consistent with the SM prediction. Taking into account the systematic uncertainty of the SES [12], the upper limit was set to $\mathcal{B}(K_L \rightarrow \pi^0\gamma) < 1.7 \times 10^{-7}$ at the 90% C.L.. This is the first experimental attempt to search for the $K_L \rightarrow \pi^0\gamma$ decay.

8. Conclusion

The $K_L \rightarrow \pi^0\gamma$ decay is forbidden by the Lorentz invariance and gauge principle. We analyzed the data collected between 2016 and 2018 and found no signal candidate in the signal region. We set the first upper limit $\mathcal{B}(K_L \rightarrow \pi^0\gamma) < 1.7 \times 10^{-7}$ at the 90% confidence level.

Acknowledgements

We are appreciate for the people of the J-PARC facility groups for their supports. We also would like to show the greatest gratitude to the KEK Computing Research Center for KEKCC. The works were supported by the Ministry of Education, Culture, Sports, Science, and Technology (MEXT) of Japan and the Japan Society for the Promotion of Science (JSPS) under the MEXT KAKENHI Grant No. JP18071006, the JSPS KAKENHI Grants No. JP23224007, No. JP16H06343, and No. JP17K05479, by the research fellowship program for postdoctoral scientists No. 17J02178, and through the Japan-U.S. Cooperative Research Program in High Energy Physics; the U.S. Department of Energy, Office of Science, Office of High Energy Physics, under Awards No. DE-SC0006497, No. DE-SC0007859, and No. DE-SC0009798; the Ministry of Education and the National Science Council/Ministry of Science and Technology in Taiwan under Grants No. 99-2112-M-002-014-MY3 and No. 102-2112-M-002-017; and the National Research Foundation of Korea (2017R1A2B2011334 and 2017R1A2B4006359).

References

- [1] Coleman S and Glashow S L 1999 *Phys. Rev. D* **59** 116008
- [2] Michimura Y *et al* 2013 *Phys. Rev. Lett.* **110** 200401
- [3] Tobar M E *et al* 2010 *Phys. Rev. D* **81** 022003
- [4] Oneda S Sasaki S and Ozaki S 1950 *Prog. Theo. Phys.* No.2 165
- [5] Merić B Kumerički K P and Trampetić J 2005 *Phys. Rev. D* **72** 057502
- [6] Buras A J *et al* 2015 *JHEP* **11** 033
- [7] Maeda Y *et al* 2015 *Prog. Theo. Exp. Phys.* **2015**, 063H01
- [8] Ahn J K *et al* 2017 *PTEP* **2017** 021C01
- [9] Lin C 2019 Kaon2019 poster

- [10] Su S *et al* 2017 *IEEE Trans. Nucl. Sci.* **64**, 1338
- [11] Olive K A *et al* 2014 *Chin. Phys. C* **38** 090001
- [12] Cousins R D and Highland V L 1992 *Nucl. Instrum. Methods A* **320** 331